Article

Nanoscale Co-organization of Quantum Dots and Conjugated Polymers Using Polymeric Micelles As Templates

Mingfeng Wang, Sandeep Kumar, Anna Lee, Neda Felorzabihi, Lei Shen, Fei Zhao, Pablo Froimowicz, Gregory D. Scholes, and Mitchell A. Winnik

J. Am. Chem. Soc., **2008**, 130 (29), 9481-9491 • DOI: 10.1021/ja801931m • Publication Date (Web): 25 June 2008

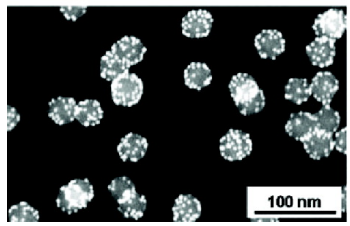

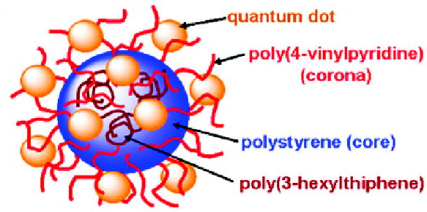

More About This Article

Additional resources and features associated with this article are available within the HTML version:

- Supporting Information
- Links to the 1 articles that cite this article, as of the time of this article download
- Access to high resolution figures
- Links to articles and content related to this article
- Copyright permission to reproduce figures and/or text from this article

View the Full Text HTML

J|A|C|S
ARTICLES

Published on Web 06/25/2008

Nanoscale Co-organization of Quantum Dots and Conjugated Polymers Using Polymeric Micelles As Templates

Mingfeng Wang, Sandeep Kumar, Anna Lee, Neda Felorzabihi, Lei Shen, Fei Zhao, Pablo Froimowicz, Gregory D. Scholes,* and Mitchell A. Winnik*

Department of Chemistry, University of Toronto, 80 St. George Street, Toronto, M5S 3H6 Ontario Canada

Received March 14, 2008; E-mail: gscholes@chem.utoronto.ca; mwinnik@chem.utoronto.ca

Abstract: Hierarchical organization of light-absorbing molecules is integral to natural light harvesting complexes and has been mimicked by elegant chemical systems. A challenge is to attain such spatial organization among nanoscale systems. Interactions between nanoscale systems, e.g., conjugated polymers, carbon nanotubes, quantum dots, and so on, are of interest for basic and applied reasons. However, typically the excited-state interactions and dynamics are examined in rather complex blends, such as cast films. A model system with complexity intermediate between a film and a supramolecular system would yield helpful insights into electronic energy and charge transfer. Here, we report a simple and versatile approach to achieving spatially defined organization of colloidal CdSe, CdSe/ZnS core/shell, or PbS nanocrystals (quantum dots) with poly(3-hexylthiophenes) (P3HTs) using micelles of poly(styrene-*b*-4-vinylpyridine) (PS-*b*-P4VP) as the main structural motif. We compare the characteristics of this system to those of natural light-harvesting complexes. Bulk heterojunction films (and related systems) are characterized by electronic interactions, and therefore dynamics of charge and energy transfer, at interfaces rather than between specific donor−acceptor molecules. Owing to structural disorder, such systems are inherently complex. Therefore, we expect that the spatially defined organization of the active components in the present system provides new opportunities for studying the complicated photophysics intrinsic to blends of nanoscale systems, such as bulk heterojunctions by establishing simplified and better controlled interfaces.

Introduction

Functional nanoscale systems, such as organic solar cells, have been the subject of much research recently largely owing to the anticipated ease of processing for producing these systems.[1–7] At the same time, it is clear that a present challenge is to elucidate the details underpinning charge and electronic energy transfer in these kinds of systems, with particular emphasis on how they differ as a direct result of their complexity from well-known donor−acceptor model systems.[8] To address these kinds of questions, it is desirable to study a model system of intermediate complexity; mimicking the features and dimensionality of bulk heterojunctions or blends, but in a better defined structure. In the present work, we report the preparation and characterization of such a system.

Prolific examples of evolutionary-directed nanoscale organization of functional chromophores can be found in natural systems. Of particular note are the photosynthetic proteins integral to light harvesting and subsequent charge separation—the primary steps in energy transduction. There are a number of well-studied examples of light-harvesting antenna proteins, for example LH2 from purple bacteria, LHCII from higher plants and algae, various phycobiliproteins from red algae and cryptophytes, or PCP from dynoflagellates.[9–14] These systems bind between about 8 up to tens of chromophores in a protein scaffold, and while the precise identity of chromophores is quite varied among these examples, the antenna systems have several important attributes in common.[15] Light may be captured anywhere in the antenna, then its energy is transferred with near unit efficiency through an "energy funnel" to the red-most electronic states of the complex. The energy gradient in this energy funnel is formed by the use of chemically different chromophores, subtle tuning of the energy of each chromophore by interaction with the local protein environment, and the use

(1) Morteani, A. C.; Dhoot, A. S.; Kim, J.-S.; Silva, C.; Greenham, N. C.; Murphy, C.; Moons, E.; Ciná, S.; Burroughes, J. H.; Friend, R. H. *Adv. Mater.* **2003**, *15*, 1708–1712.
(2) Beek, W. J. E.; Wienk, M. M.; Janssen, R. A. J. *J. Mater. Chem.* **2005**, *15*, 2985–2988.
(3) Huynh, W. U.; Dittmer, J. J.; Alivisatos, A. P. *Science* **2002**, *295*, 2425–2427.
(4) Peumans, P.; Uchida, S.; Forrest, S. R. *Nature* **2003**, *425*, 158–162.
(5) Koeppe, R.; Sariciftci, N. S. *Photochem. Photobiol. Sci.* **2006**, *5*, 1122–1131.
(6) Hoppe, H.; Sariciftci, N. S. *J. Mater. Res.* **2004**, *19*, 1924–1945.
(7) Nelson, J. *Curr. Opin. Solid State Mater. Sci.* **2002**, *6*, 87–95.
(8) Scholes, G. D.; Rumbles, G., *Excitons in Nanoscale Systems: Fundamentals and Applications*. World Scientific: Singapore, 2007; Vol. 2, pp 103−157.
(9) Grondelle, R. V.; Dekker, J. P.; Gillbro, T.; Sundström, A. V. *Biochim. Biophys. Acta* **1994**, *1187*, 1–65.
(10) Amerongen, H. V.; Valkkunas, L.; Grondelle, R. V., *Photosynthesis Excitons*. World Scientific: Singapore, 2000.
(11) Sundström, V.; Pullertis, T.; Grondelle, R. V. *J. Phys. Chem. B* **1999**, *103*, 2327–2346.
(12) Scheer, H. *Angew. Chem., Int. Ed. Engl.* **1981**, *20*, 241–261.
(13) Glazer, A. N. *J. Biol. Chem.* **1989**, *264*, 1–4.
(14) Fetisova, Z. G.; Frieberg, A. M.; Timpmann, K. E. *Nature* **1988**, *334*, 633–634.
(15) Scholes, G. D.; Fleming, G. R. *Adv. Chem. Phys.* **2005**, *132*, 57–129.

Chart 1. Schematic Presentation of the Self-Assembly of PS_{404}-*b*-$P4VP_{76}$ Diblock Copolymer, P3HT, and CdSe/TOPO QDs into Composite Micelles in which P3HT Chains Are in the Core and QD Particles Are in the Corona

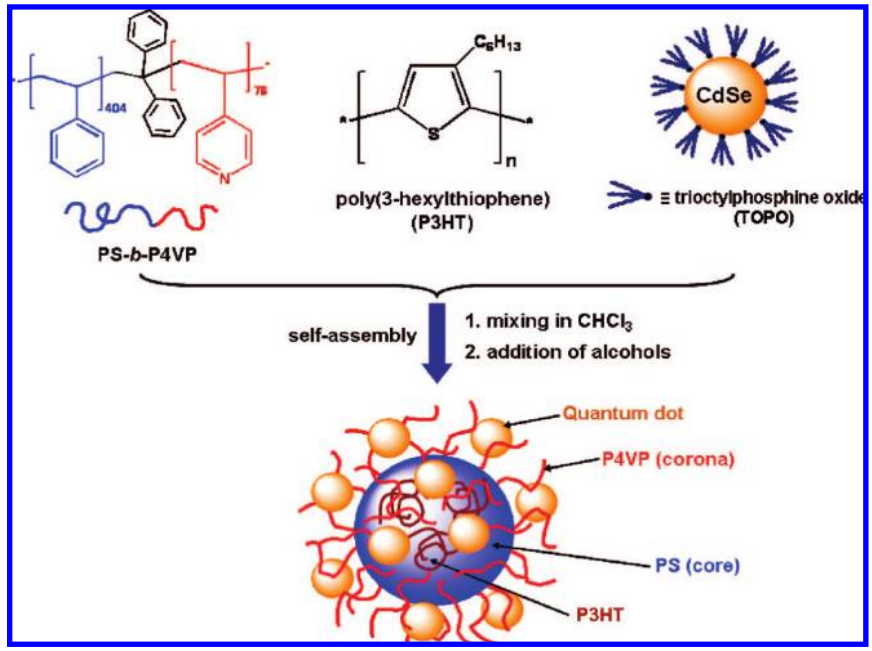

of interactions among chromophores in aggregate motifs.[16] Here, we report an example of a synthetic system that displays these kinds of structural features. However, a crucial difference is that the "chromophores" in our system are nanoscale objects (quantum dots (QDs) and conjugated polymers), so overall, the complex is many times larger than natural light harvesting systems. This opens up the possibility that electronic energy flow and its relationship to the organization of nanoscale building blocks can be studied. Important previous work has explored electronic energy transfer and even directed light-harvesting in layer-by-layer assembled thin solid films of nanocrystalline QDs.[17–20] Here, we demonstrate the use of a micellar scaffold that contains specific domains into which conjugated polymer and nanocrystalline QDs can be partitioned.

Specifically, we report a simple and versatile approach to achieving spatially defined organization of colloidal CdSe, CdSe/ZnS core/shell, or PbS QDs with poly(3-hexylthiophenes) (P3HTs) using micelles of poly(styrene-*b*-4-vinylpyridine) (PS-*b*-P4VP) as the main structural motif. This polymer forms spherical micelles when dissolved in a variety of different alcohols such as 1-butanol (n-BuOH) or 2-propanol (2-PrOH) and in mixtures of chloroform and methanol. These micelles, with a PS core and a P4VP corona, have two properties of interest. First, they can solubilize P3HT in the PS core due to their similar solubility parameters and their common insolubility in the solvents. Second, they can bind a variety of different QDs within the coronae because of favorable interaction with the P4VP block. This creates a spatial organization that may allow electronic energy transfer (EET) and/or photoinduced charge transfer (PCT) between the QDs and P3HT. This paper reports steady-state fluorescence measurements that demonstrate excited-state interactions between the QDs and the conducting polymer. Our approach provides an opportunity for preparing a variety of composite materials with both multiple functions and hierarchical ordered structures that mimic these structural characteristics of light harvesting complexes in nature.

Results and Discussion

The basic idea behind the experiments described here is that "crew-cut" block copolymer micelles[21] formed by poly(styrene-*b*-4-vinylpyridine) (PS-*b*-P4VP) in alcohol solvents can serve as a scaffold for organizing the spatial arrangement of CdSe quantum dots and poly(3-hexylthiophene) (P3HT), a conducting polymer. Crew-cut micelles are formed from block copolymers in which the insoluble block (here PS) is much longer than the soluble block (here P4VP), leading to a structure in which uniform spheres of PS are surrounded by short, stubby "hairs" of P4VP. The role of the scaffold is to hold the QDs and P3HT in close proximity, but to maintain them in separate phases. In the structures we describe below, the conducting polymer is confined to the PS core of the micelle, and the QDs become integrated into the P4VP corona of the micelle. Because the P4VP chains are short, the QDs are held close (1 to 2 nm) to the PS surface, which should enable energy or electron transfer between these components. A drawing of the desired nanocomposite structure and the structures of the polymer and quantum dot building blocks is presented in Chart 1.

QDs were synthesized by traditional high-temperature methods in organic media in the presence of organic surfactants as stabilizers. QDs synthesized in this way are normally single crystals, similar in shape, and nearly monodisperse in size. They are characterized by a well-defined band-edge absorption peak, a narrow photoluminescence (PL) spectrum, and a substantial PL quantum yield. For the CdSe QDs that we employ, this synthesis approach leads to a layer of surface ligands of

(16) Fleming, G. R.; Scholes, G. D. *Nature* **2004**, *431*, 256–257.
(17) Crooker, S. A.; Hollingsworth, J. A.; Tretiak, S.; Klimov, V. I. *Phys. Rev. Lett.* **2002**, *89*, 186802.
(18) Kagan, C. R.; Murray, C. B.; Nirmal, M.; Bawendi, M. G. *Phys. Rev. Lett.* **1996**, *76*, 1517–1520.
(19) Franzl, T.; Koktysh, D. S.; Klar, T. A.; Rogach, A. L.; Feldmann, J.; Gaponik, N. *Appl. Phys. Lett.* **2004**, *84*, 2904–2906.
(20) Franzl, T.; Klar, T. A.; Schietinger, S.; Rogach, A. L.; Feldmann, J. *Nano Lett.* **2004**, *4*, 1599–1603.
(21) Hernández, J. R.; Chécot, F.; Gnanou, Y.; Lecommandoux, S. *Prog. Polym. Sci.* **2005**, *30*, 691–724.

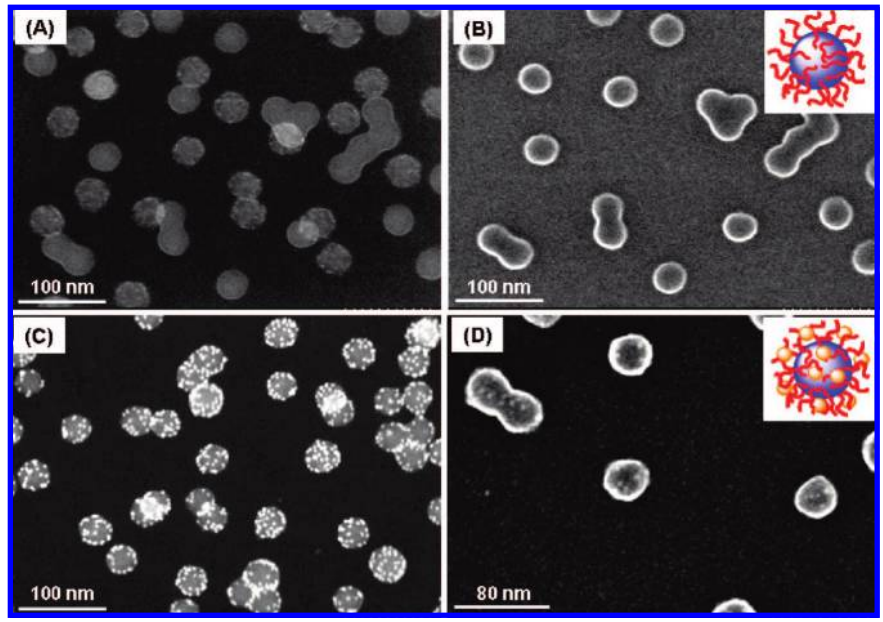

Figure 1. TEM (A, C) and SEM (B, D) images of PS_{404}-*b*-$P4VP_{76}$ micelles prepared in *n*-BuOH (A, B) and the corresponding micelles bearing CdSe(559) QDs (C, D). The concentration of the block copolymer was 0.25 mg/mL in each case. The QD concentration for the sample in (C, D) was 5.0×10^{-7} M. Insets (B, D): the structure models of the crew-cut polymeric micelles before and after the attachment of the QDs.

trioctylphosphine and trioctylphosphine oxide, which we collectively refer to as TOPO. P4VP serves as a multidentate ligand[22] to assist in the transfer of these QDs to polar media such as alcohols. It is well-known that pyridine groups are effective at displacing TOPO from the surface of these kinds of QDs.[23,24]

To put our work in context, we note that a variety of different approaches have been used to create colloidal nanocomposites of synthetic polymers or block copolymer micelles and inorganic nanoparticles. For example, some groups have used block copolymer micelles[25–27] or cylindrical polymer brushes[28] as templates for the growth of metal or semiconductor nanoparticles (NPs). For example, CdS QDs formed in the poly(acrylic acid) domain of poly(styrene-*b*-acrylic acid) (PS-*b*-PAA) micelles by this method typically showed a broad PL spectrum with a rather low band-edge PL intensity and a substantial trap-state emission.[27] Other groups have been concerned with strategies such as encapsulation for transferring QDs into polar media or into water. For example, single or multiple QDs have been encapsulated into the hydrophobic cores of surfactant micelles[29] or shell-cross-linked polymer micelles[30] in water. We have used polymers with dimethylaminoethyl-pendant groups for transferring CdSe/TOPO into polar media and into water via a process involving ligand exchange.[33]

One of the major objectives of the study of self-assembly is to learn how to construct complex nanostructures in a simple manner.[34] Our design for the construction of the colloidal nanocomposite structure depicted in Chart 1 is to dissolve the various components in a common good solvent (chloroform), and then add a selective solvent (an alcohol) to induce self-assembly. If the building blocks are chosen appropriately, then they will partition during microphase separation to yield the desired structure. To meet this objective, one needs to understand how the individual components interact in chloroform and in the presence of the second solvent. In the sections that follow, we describe these interactions, and show how they lead naturally to the integrated structure presented in Chart 1. These experiments employ a single sample of PS_{404}-*b*-$P4VP_{76}$ ($M_n = 50{,}100$, $M_w/M_n = 1.1$, where the subscripts refer to the number average degree of polymerization). While the emphasis of this paper is on structure formation, we also report preliminary absorbance and steady-state photoluminescence experiments that show that within the structure, excited-state communication (energy or charge transfer) can occur between the photoactive components.

PS-*b*-P4VP Micelles. When various alcohol solvents were added to solutions of PS_{404}-*b*-$P4VP_{76}$ in chloroform, at concentrations on the order of 1.0 mg/mL, spherical crew-cut micelles formed. For *n*-BuOH and 2-PrOH as the selective solvent, the micelle solutions remained colloidally stable after removal of the $CHCl_3$ with a rotary evaporator, whereas with methanol, micelles formed for volume ratios ranging from 1:2 to 1:4 ($CHCl_3$:methanol). Figure 1, parts A and B, shows transmission and scanning electron microscopy (TEM, SEM) images, respectively, of PS-*b*-P4VP micelles formed in *n*-BuOH. These spherical micelles appear uniform in size and shape. Some aggregated structures can be seen in the images. These formed during solvent evaporation on the TEM grid. No evidence of aggregation was detected by dynamic light scattering (see below). From analysis of approximately 100 individual micelles,

(22) Wang, X.-S.; Dykstra, T. E.; Salvador, M. R.; Manners, I.; Scholes, G. D.; Winnik, M. A. *J. Am. Chem. Soc.* **2004**, *126*, 7784–7785.
(23) Kuno, M.; Lee, J. K.; Dabbousi, B. O.; Mikulec, F. V.; Bawendi, M. G. *J. Chem. Phys.* **1997**, *106*, 9869–9882.
(24) Skaff, H.; Emrick, T. *Chem. Commun.* **2003**, 52–53.
(25) Moffitt, M.; McMahon, L.; Pessel, V.; Eisenberg, A. *Chem. Mater.* **1995**, *7*, 1185–1192.
(26) Förster, S.; Antonietti, M. *Adv. Mater.* **1998**, *10*, 195–217.
(27) Wang, C.-W.; Moffitt, M. G. *Langmuir* **2004**, *20*, 11784–11796.
(28) Zhang, M.; Drechsler, M.; Muller, A. H. E. *Chem. Mater.* **2004**, *16*, 537–543.
(29) Dubertret, B.; Skourides, P.; Norris, D. J.; Noireaux, V.; Brivanlou, A. H.; Libchaber, A. *Science* **2002**, *298*, 1759–1762.
(30) Kim, B.-S.; Taton, T. A. *Langmuir* **2007**, *23*, 2198–2202.
(31) Wang, M.; Dykstra, T. E.; Lou, X.; Salvador, M. R.; Scholes, G. D.; Winnik, M. A. *Angew. Chem., Int. Ed.* **2006**, *45*, 2221–2224.
(32) Wang, M.; Oh, J. K.; Dykstra, T. E.; Lou, X.; Scholes, G. D.; Winnik, M. A. *Macromolecules* **2006**, *39*, 3664–3672.

we calculate an average diameter $d = 40.7 \pm 2.8$ nm. With 2-PrOH as the added alcohol, $d = 33.9 \pm 2.7$ nm, whereas in a mixture of chloroform/methanol (1:2, v/v), $d = 28.7 \pm 3.1$ nm. These differences are likely due to differences in the solvency of the medium for polystyrene during self-assembly. Swelling of the core by solvent would reduce the repulsion between corona chains and lead to larger aggregation numbers for the micelles. Returning to the image in Figure 1A, we note that it is not possible to discern contrast between the PS core and the thin P4VP shell. P4VP represents approximately 16 vol % of the polymer in the bulk state. On the basis of this composition, we estimate that the P4VP shell contributes about 6% to the measured particle diameter. Thus, for the micelles seen in the TEM, the collapsed P4VP corona contributes a shell 1.2-nm thick for micelles formed in *n*-BuOH and 1.0 nm for micelles formed in 2-PrOH.

QD/PS-b-P4VP Hybrid Micelles. In order to test whether the P4VP corona of these spherical micelles could act as an anchoring domain for CdSe QDs, we mixed a solution of the block copolymer in chloroform with a solution of purified CdSe(559)/TOPO QDs and then added *n*-BuOH as a precipitant for the PS block. Figure 1, parts C and D, shows TEM and SEM images, respectively, obtained from solutions in *n*-BuOH after removal of most of the chloroform by rotary evaporation. These images show that the QDs are bound to the surface of the micelles, presumably through attachment to the P4VP chains that formed the micelle corona. No free QDs can be observed, indicating the high efficiency of the QD binding to the corona-forming polymer. It is important to note that the QDs used here do not require any pretreatment of their surfaces. This method is in contrast to previous approaches of dispersing metal or semiconductor nanoparticles (NPs) into one phase of a block copolymer matrix, in which surface modification of the NPs was required to enhance selective compatibility.[35,36]

As determined by TEM, the average diameter (38.2 ± 2.1 nm) of the micelles obtained in the presence of the QDs was slightly (3 nm) smaller than the size of the bare micelles formed with *n*-BuOH. A complicating feature of size determination via SEM and TEM images is that the QDs at the surface of the particles impart some nonuniformity to the particle shape and contribute to the measured diameter. As in the case of the block copolymer itself, micelle formation is driven by the insolubility of PS in *n*-BuOH. It is in some ways remarkable that the micelle size is so little affected by the presence of the QDs. One might expect that the details of the solvent-induced self-assembly process would be perturbed by the interaction of the QDs bound with the P4VP chains. What one sees is that this perturbation is much smaller than that caused by a change in nonsolvent used to induce micelle formation. In order to obtain a better understanding QD binding to the micelle corona, we next consider how these CdSe/TOPO QDs interact with polyvinylpyidine homopolymer in chloroform solution.

Comparison of Interaction of P2VP and P4VP with CdSe QDs. There are two common constitutional isomers of polyvinylpyridine, poly(2-vinylpyridine) (P2VP) and P4VP. They differ in the respective steric accessibility of their nitrogen atoms. Since pyridine has been used as a ligand to displace TOPO from CdSe/TOPO QDs,[23,24] one might anticipate that both polymers would interact effectively with CdSe/TOPO. Surprisingly, the nature of the interaction of QDs with pyridine-based polymers is still poorly understood, and seemingly contradictory results were recently reported for the location of CdSe/TOPO QDs in PS-*b*-P2VP films.[37,38] We tested the ability of P2VP and P4VP to act as a multidentate ligand[22,31–33] for CdSe/TOPO QDs by combining the materials in $CHCl_3$, a common solvent for the polymers and for the QDs. When solutions of CdSe(559)/TOPO and excess P4VP were stirred at 23 °C for 16 h, the particles obtained were insoluble in hexane, a good solvent for CdSe/TOPO, but could be dispersed in methanol, in which CdSe/TOPO is completely insoluble. A similar solubility change was observed for PbS/OA QDs after treatment in $CHCl_3$ with excess P4VP. We infer that P4VP bound to the QD surface displaces a sufficient number of TOPO or OA groups to render the QDs soluble in polar solvents. In contrast, the efficiency (<30%) of transferring these QDs into methanol using P2VP was much lower, despite the similar solubility of P2VP and P4VP in methanol, likely due to the steric restriction for the binding to P2VP. This result suggests that P2VP has a weaker interaction with the QDs.

The pretreatment of CdSe QDs with the two different polyvinylpyridine isomers in chloroform had different effects on the organization of QDs with respect to the PS_{404}-*b*-$P4VP_{76}$ micelles formed when alcohol was added to the mixture. For example, when a solution of P4VP-saturated QDs was mixed with PS-*b*-P4VP in $CHCl_3$ followed by addition of methanol ($CHCl_3$:methanol = 1:2, v/v), the TEM result (Figure 2A) shows no interaction between the QDs and the micelles. In contrast, when a $CHCl_3$ solution of QDs pretreated with P2VP was mixed with PS-*b*-P4VP under the same conditions, complete transfer of the QDs to the P4VP corona of the micelles took place (Figure 2B). As shown in the Supporting Information (Figure S3), very similar results were obtained when these experiments were repeated using 2-PrOH as the nonsolvent for PS. Taken together, these results indicate that P4VP binds more strongly than P2VP to the CdSe QDs, and that once P4VP homopolymer binds to the QDs, it is difficult for it to be displaced by P4VP chains of the PS-*b*-P4VP block copolymer. We also infer that in the formation of the micelles depicted in Figure 1, parts C and D, P4VP blocks adsorb to the QD surface prior to phase separation induced by addition of the selective solvent.

Effect of QD Composition on Micelle Formation. In this section, we examine the generality of the self-assembly process by extending experiments to include PbS quantum dots (that emit in the near-infrared region) and CdSe/ZnS core−shell quantum dots. These experiments were carried out with 2-PrOH as the solvent to induce micelle formation. Figure 3B shows the TEM image of the micelles formed in 2-PrOH in the presence of CdSe(559)/TOPO QDs. The polymer concentration was 0.25 mg/mL with 5.7×10^{-7} M QDs. As in the case of butanol, all of the QDs were adsorbed onto the micelles. The mean diameter of the QD−micelle composites determined from the TEM image was 31.5 ± 2.7 nm, very similar to that of the bare micelles $d = 33.9 \pm 2.7$ nm (Figure 3A).

(33) Wang, M.; Felorzabihi, N.; Guerin, G.; Haley, J. C.; Scholes, G. D.; Winnik, M. A. *Macromolecules* **2007**, *40*, 6377–6384.
(34) Zhong, S.; Cui, H.; Chen, Z.; Wooley, K. L.; Porchan, D. J. *Soft Matter* **2008**, *4*, 90–93.
(35) Bockstaller, M. R.; Michiewicz, R. A.; Thomas, E. L. *Adv. Mater.* **2005**, *17*, 1331–1349.
(36) Balazs, A. C.; Emrick, T.; Russell, T. P. *Science* **2006**, *314*, 1107–1110.
(37) Zou, S.; Hong, R.; Emrick, T.; Walker, G. C. *Langmuir* **2007**, *23*, 1612–1614.
(38) Lin, Y.; Boker, A.; He, J.; Sill, K.; Xiang, H.; Abetz, C.; Li, X.; Wang, J.; Emrick, T.; Long, S.; Wang, Q.; Balazs, A.; Russell, T. P. *Nature* **2005**, *434*, 55–59.

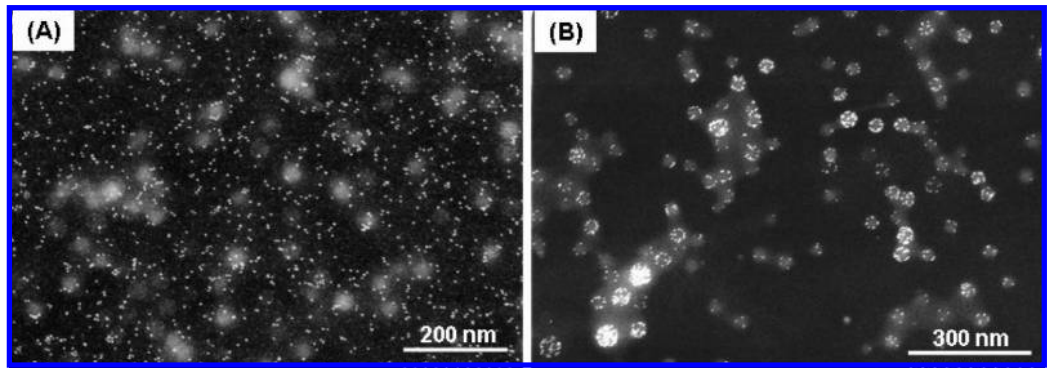

Figure 2. TEM images of CdSe-559 QDs (in 1.0 mL of $CHCl_3$, 1.8×10^{-6} M) pre-treated with (A) P4VP (14.0 mg) or (B) P2VP (11.0 mg) to which PS_{404}-*b*-$P4VP_{76}$ (in 1.0 mL of $CHCl_3$, 1.0 mg/mL) was added, and then micelle formation was induced by adding MeOH (4.0 mL). Panel A shows a mixture of free QDs plus micelles, whereas panel B shows that all of the QDs are bound to the coronae of the micelles.

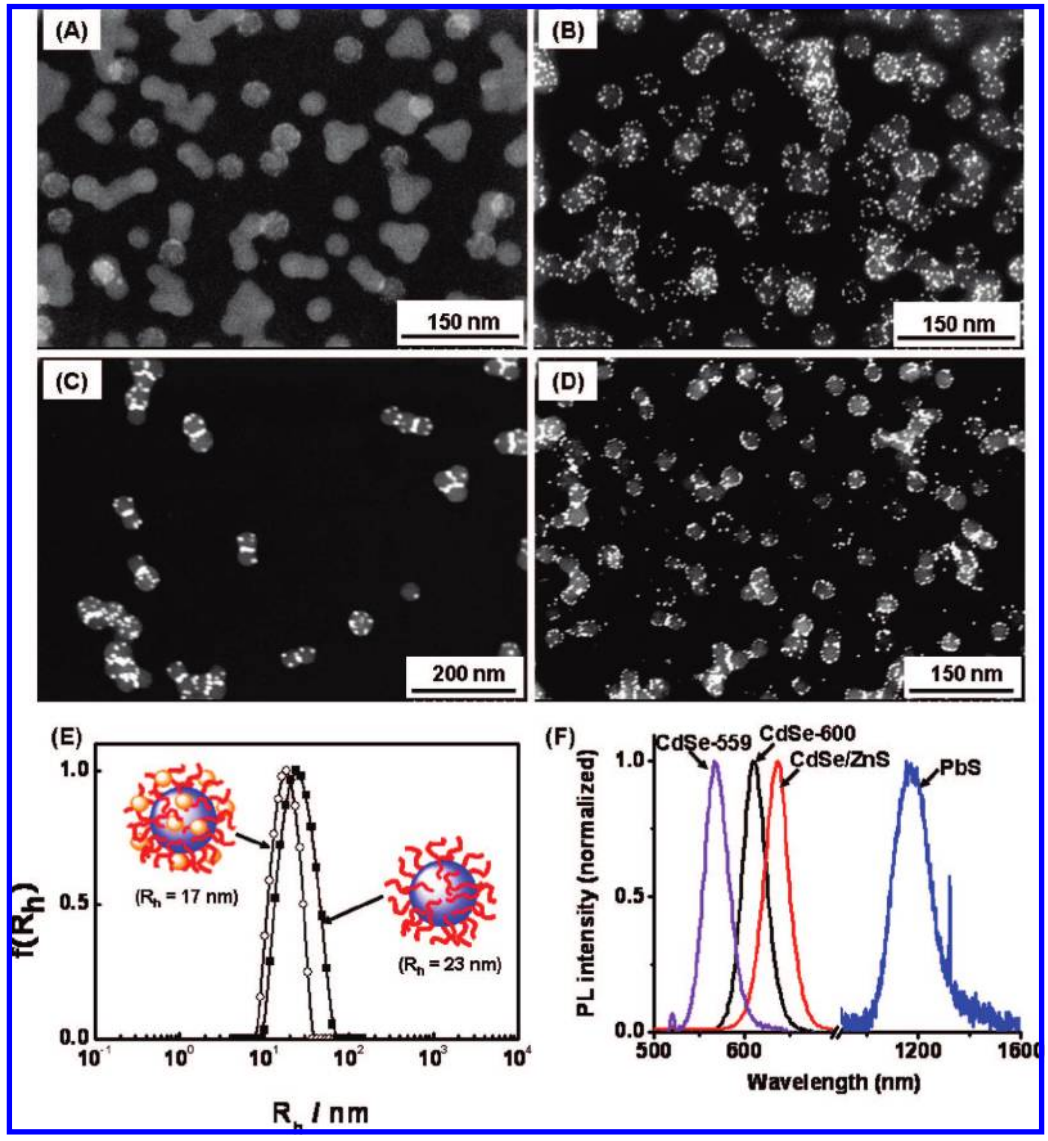

Figure 3. (A−D) TEM images of PS_{404}-*b*-$P4VP_{76}$ micelles (0.25 mg/mL) obtained from 2-PrOH solution (A) in the absence of QDs and in the presence of (B) CdSe(559) QDs (5.7×10^{-7} M), (C) CdSe/ZnS core/shell QDs (0.25 mg/mL), and (D) PbS QDs (0.13 mg/mL). (E) DLS traces (CONTIN plots) of PS_{404}-*b*-$P4VP_{76}$ micelles QDs in 2-PrOH prepared in the presence of and in the absence of CdSe(559). (F) PL spectra of the various QDs attached to the coronae of PS-*b*-P4VP micelles in 2-PrOH.

Dynamic light scattering (DLS) measurements (Figure 3E) indicated a monomodal and narrow size distribution of species in solution, with a hydrodynamic radius (R_h) of 23 nm and a polydispersity (PDI) of 0.10 for the bare micelles, larger than the hard-sphere radius (16 nm) determined by TEM. This difference is due to swelling of the P4VP corona chains in

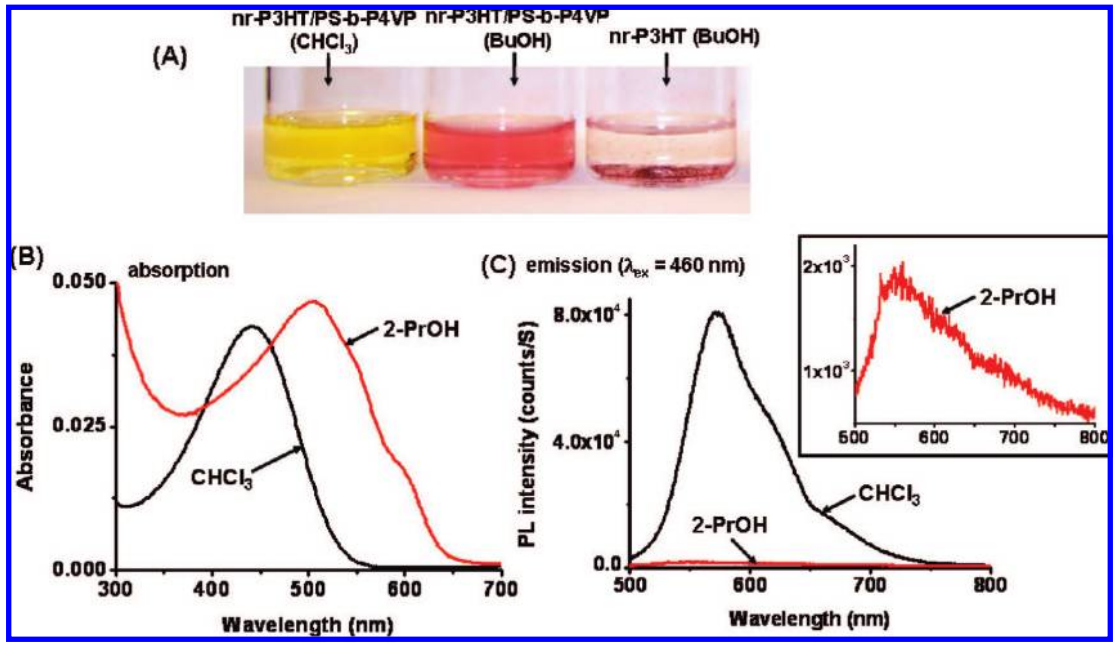

Figure 4. (A) Digital photographs of *nr*-P3HT/PS_{404}-*b*-$P4VP_{76}$ in $CHCl_3$, *n*-BuOH, and *nr*-P3HT in *n*-BuOH. (B) Absorption and (C) emission spectra of P3HT/PS_{404}-*b*-$P4VP_{76}$ in $CHCl_3$ and 2-PrOH, respectively. The inset in C presents the enlarged emission spectrum of P3HT/PS_{404}-*b*-$P4VP_{76}$ in 2-PrOH.

2-PrOH, and suggests that the thickness of the solvent-swollen corona layer is on the order of 7 nm. When these micelles were formed in the presence of CdSe(559)/TOPO, the DLS size distribution still appeared narrow (PDI = 0.09), and the hydrodynamic radius became smaller. The value of R_h = 17 nm implies that in 2-PrOH solution, the corona laden with QDs extends only 1 to 2 nm from the PS core.

Under the same conditions used to prepare CdSe(559)/PS_{404}-*b*-$P4VP_{76}$ hybrid micelles in 2-PrOH, analogous structures could be prepared with the slightly larger CdSe(600)/TOPO QDs (Figure S4, Supporting Information), with hexadecylamine (HDA)-stabilized core/shell CdSe/ZnS QDs (Figure 3C), and with oleic acid-stabilized PbS(1100)/OA QDs (Figure 3D). One difference in the case of PbS/OA QDs is that the block copolymer does not capture all of the QDs added to the solution. The TEM image of the micelles formed in 2-PrOH shows a small fraction of free QDs. One reason for this difference is that the PbS/OA QDs themselves are soluble in the medium: they remain in solution when excess butanol or 2-propanol is added to a chloroform solution of the QDs. In contrast, both CdSe/TOPO and CdSe/ZnS/HDA QDs precipitate in 2-propanol under similar conditions. Figure 3F shows the normalized photoluminescence (PL) spectra of the various QD-hybrid micelles in 2-PrOH. The emission spectra of the QDs do not change significantly for the micelle-bound QDs in 2-PrOH compared with the original QDs in $CHCl_3$. These results open the possibility for creating micelle−QD hybrid structures containing mixtures of QDs of different sizes or different compositions within the corona of a single polymer micelle. This is a topic we hope to investigate in the future.

Polythiophene/PS-*b*-P4VP Hybrid Micelles. We next consider the incorporation of poly(3-hexylthiophene) (P3HT) as an example of a conjugated polymer into the PS_{404}-*b*-$P4VP_{76}$ micelles. The idea that P3HT and PS might be compatible or even molecularly miscible comes from the work of Yu and co-workers,[39,40] who reported that oligo-3-alkylthiophene-polystyrene block copolymers did not undergo microphase separation in the bulk state. These authors explained this result by showing that the two types of polymers had similar solubility parameters. To prepare the micelles, a regiorandom P3HT (*nr*-P3HT) (M_n = 42 000, 0.2 mL, 0.5 mg/mL in $CHCl_3$) was chosen first to mix with PS_{404}-*b*-$P4VP_{76}$ (1.0 mL, 1.0 mg/mL, in $CHCl_3$) resulting in a bright yellow solution. Upon addition of 2-PrOH or *n*-BuOH (4 mL) under gentle shaking, the solution turned pink, and remained clear and pink as the $CHCl_3$ was removed by rotary evaporation. In contrast, when this experiment was repeated in the absence of PS-*b*-P4VP, the P3HT formed a purple precipitate, leaving a nearly colorless solution in the vial (Figure 4A). This result is consistent with the insolubility of P3HT in polar solvents such as 2-PrOH. The color change of P3HT from $CHCl_3$ to the micelle solution in 2-PrOH reflects the red shift of the absorbance maximum from 440 to 500 nm, accompanied by a blue shift of the PL peak from 570 to 550 nm as well as a large decrease (>99%) in PL intensity (Figure 4). These spectroscopic changes are indicative of the formation of P3HT aggregates within the micelle.[41–43]

For a fixed amount (1.0 mg) of PS_{404}-*b*-$P4VP_{76}$ in 4 mL 2-PrOH, the maximum amount of P3HT that could be incorporated into the micelles, based upon visual inspection, was 1.3 mg. Below this limit, clear colored solutions were obtained that could be passed through a 0.2-μm filter with little loss of P3HT material. The color became darker (from pink to dark brown) with an increase of P3HT concentration. However, when the amount of P3HT added was higher than 1.3 mg per mg micelle (e.g., 2.5 mg), turbid solutions or even a purple precipitate were observed. More quantitative information about the incorporation of P3HT into the micelles was obtained by DLS and TEM. Figure 5 presents CONTIN plots from DLS

(39) Li, W.; Maddux, T.; Yu, L. *Macromolecules* **1996**, *29*, 7329–7334.
(40) Li, W.; Wang, H.; Yu, L.; Morkved, T. L.; Jaeger, H. M. *Macromolecules* **1999**, *32*, 3034–3044.
(41) Leclerc, M. *Adv. Mater.* **1999**, *11*, 1491–1498.
(42) Jenekhe, S. A.; Chen, X. L. *J. Phys. Chem. B* **2000**, *104*, 6332–6335.
(43) Magnani, L.; Rumbles, G.; Samuel, I. D. W.; Murray, K.; Moratti, S. C.; Holmes, A. B.; Friend, R. H. *Synth. Met.* **1997**, *84*, 899–900.

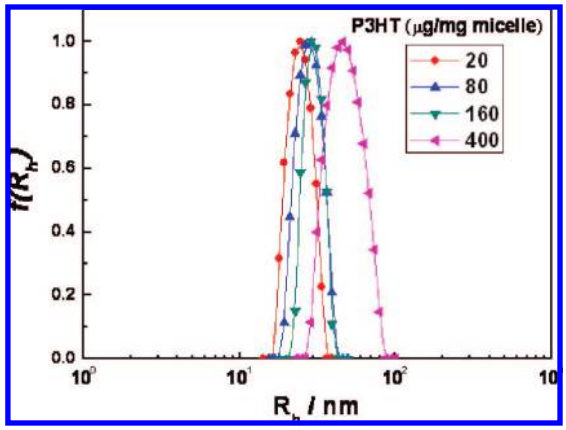

Figure 5. CONTIN plots of the hydrodynamic radius distribution from DLS measurements on PS_{404}-*b*-$P4VP_{76}$ micelles with different amounts of *nr*-P3HT incorporated. The concentration of PS_{404}-*b*-$P4VP_{76}$ in 2-PrOH for all the samples is the same (0.25 mg/mL). All of the samples were filtered with a 0.2-μm filter before the characterization.

measurements on solutions in 2-propanol of the micelles with different amounts of P3HT incorporated. With an increase of P3HT from 20 to 160 μg/mg micelle, small increases in R_h (24.6 to 29.5 nm, PDI = 0.01 to 0.07) were observed, compared with the values of the micelles without P3HT (R_h =23.7 nm, PDI = 0.1). When the amount of P3HT was increased to 400 μg/mg micelle, the R_h increased dramatically (to 45.9 nm) accompanied by an increase of the PDI to 0.17. Here, the formation of aggregates may be the cause of this dramatic increase in R_h. The TEM images (Figure S5, Supporting Information) also show clusters of micelles, but it is difficult to tell if the clusters were present in solution or were formed as the solvent evaporated. From size analysis of these TEM images, the mean diameter of the individual micelles was 27.9 $\pm$ 2.2 nm for the sample containing 20 μg P3HT/mg micelle and 30.9 $\pm$ 2.9 nm for 400 μg P3HT/mg micelle, similar to the diameter (33.9 $\pm$ 2.7 nm) of the PS_{404}-*b*-$P4VP_{76}$ micelles themselves.

Using this procedure, we were also able to incorporate a low molar mass sample (M_n = 10 000, M_w/M_n = 1.2) of regioregular P3HT (rr-P3HT) into the polymeric micelles (Figure S6, Supporting Information). The absorption spectrum of *rr*-P3HT in the polymeric micelles shows more structure (with maxima at 517, 550, and 600 nm) than that of the regiorandom analogue. As in the case of *nr*-P3HT, *rr*-P3HT in PS_{404}-*b*-$P4VP_{76}$ micelles in 2-PrOH exhibited a weak and broad fluorescence in the range of 600−800 nm, strongly quenched compared with the corresponding fluorescence in $CHCl_3$.[43]

The results described above demonstrate the encapsulation of P3HT by PS_{404}-*b*-$P4VP_{76}$ micelles. DLS measurements indicate that there is no significant influence of P3HT on the micelle size and size distribution even for 160 μg P3HT per mg micelle. We infer that the P3HT is preferentially located in the PS core of the micelles. It is more difficult to know the extent of miscibility of P3HT in the PS phase. We know on one hand that the two polymer have similar solubility parameters.[39,40] Liu et al.[44] have reported that *rr*-P3HT-PS diblock copolymers undergo phase separation when thick films were prepared by free evaporation of toluene from drop-cast films, but no phase separation could be discerned by AFM for thin films spin-coated from chloroform. This result suggests that phase separation may be driven by the crystallization of the *rr*-P3HT. Babel and Jenekhe[45] presented clear evidence for phase separation in spin-coated films of PS/*rr*-P3HT blends, but the molecular weights of their samples were much higher than those of the other authors cited above. In our experiments, the color shift and strong fluorescence quenching is an indication of aggregation of P3HT molecules. It is not possible at the present time to know if this indicates full or partial phase separation within the micelle core. Experiments to be described below indicate that the P3HT encapsulated in the micelles is able to quench the photoluminescence of CdSe QDs bound to the corona. We take this result to mean that at least some of the P3HT is located in the surface region of the micelle core.

Structural Characterization of QD/Polythiophene/PS-*b*-P4VP Hybrid Micelles. We next turn our attention to preparation of hybrid structures containing P3HT in the PS_{404}-*b*-$P4VP_{76}$ micelle core and CdSe QDs in the corona. For spectroscopic reasons, we chose *nr*-P3HT as the conjugated polymer and CdSe(600)/TOPO as the QDs. This polymer−QD pair has maximum emission intensities that are better separated than in combinations involving *rr*-P3HT. To avoid the possibility of intermicellar aggregation at a high amount of P3HT per micelle, we chose a ratio of 100 μg P3HT per mg PS_{404}-*b*-$P4VP_{76}$. To prepare the ternary hybrid micelles, 0.2 mL of nr-P3HT (0.5 mg/mL in $CHCl_3$, containing 2.38 $\times$ 10^{-9} mole polymer) and 1.0 mL of PS_{404}-*b*-$P4VP_{76}$ (1.0 mg/mL in $CHCl_3$) were mixed first. Then various amounts of CdSe(600)/TOPO (0.2 to 1.0 mL, 0.2 mg/mL (2.8 $\times$ 10^{-6} M) in $CHCl_3$) were added, followed by addition of 2-PrOH (4 mL). After removal of $CHCl_3$ (together with some 2-PrOH) on a rotary evaporator, the final volume of the solutions was adjusted to 8 mL with 2-PrOH. Figure 6 shows that these samples all formed uniform spherical micelles with the QDs incorporated exclusively in the corona. In Figure 6, parts A and B, we show TEM and SEM images of the sample containing 40 μg QDs/mg block copolymer. The presence of both P3HT and the QDs does not appear to have a significant influence on the micelle size (d = 33.6 $\pm$ 3.5 nm, Figure 6A) compared with the size of the bare PS_{404}-*b*-$P4VP_{76}$ micelles in 2-PrOH (d = 33.9 $\pm$ 2.7 nm, Figure 3A). Figure 6, parts C,D and E,F, shows corresponding images of the micelles containing the same amounts of P3HT and block copolymer, but increasing amounts of QDs.

By visual inspection of the images in Figure 6, we see that the average number of QDs incorporated into each micelle increases with the increase of QD concentration. At a small ratio of QDs/micelle, there is no indication of significant agglomeration of micelles. The solutions are transparent, and the TEM and SEM images resemble those of the QD-containing micelles described above. At higher loading of QDs (e.g., 200 μg QD/mg block copolymer) the solutions become noticeably turbid, and the contribution of light scattering can be seen in their UV−vis absorption spectra (e.g., Figure S10, Supporting Information). In addition, the TEM and SEM images (Figure 6, parts E and F) show clear evidence for agglomeration of micelles. We can imagine three factors that might promote this agglomeration. First, there may be bridging aggregation in which some quantum dots are bound to corona chains of adjacent micelles. Second, with an increasing ratio of QDs to micelles, the P4VP brushes may collapse and provide less steric stabilization. Alternatively, since the experiments were carried out at

(44) Liu, J. S.; Sheina, E.; Kowalewski, T.; McCullough, R. D. *Angew. Chem., Int. Ed.* **2002**, *41*, 329–332.

(45) Babel, A.; Jenekhe, S. A. *Macromolecules* **2004**, *37*, 9835–9840.

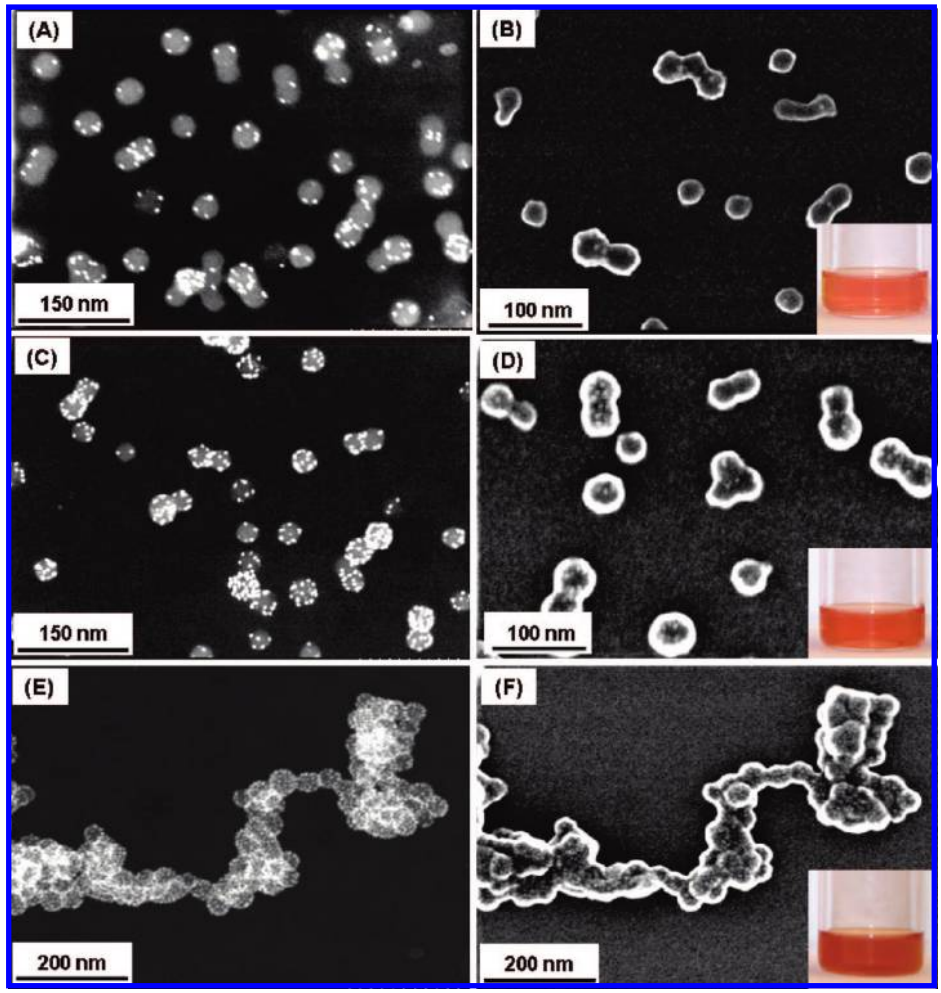

Figure 6. TEM (left panel: A, C, E) and SEM (right panel: B, D, F) images of samples prepared from ternary mixtures of P3HT, CdSe(600)/TOPO and PS_{404}-*b*-$P4VP_{76}$ from 2-PrOH solutions of micelles containing different amounts (A,B: 40 μg; C,D: 100 μg; E,F: 200 μg) of QDs per mg of the block copolymer. The concentrations of PS_{404}-*b*-$P4VP_{76}$ and P3HT were 0.12 and 0.01 mg/mL, respectively, in each sample. The insets in (B), (D), and (F) show digital photographs of the solutions from which the samples were taken.

constant block copolymer concentration, QDs at the exterior of the micelle may have had fewer TOPO ligands displaced, leading to some QD aggregation. These aggregates represent a kind of higher order of self-assembly in the system.

Spectroscopic Characterization of QD/Polythiophene/PS-*b*-P4VP Hybrid Micelles. We carried out steady-state fluorescence measurements with the objective of testing for photoinduced communication (energy transfer or electron transfer) between the CdSe QDs and the P3HT polymer within the hybrid nanostructures formed by self-assembly. The micelles and micelle-hybrids employed were prepared in 2-PrOH at a concentration of 0.25 mg/mL. The fully integrated nanocomposite contained 100 μg each of *nr*-P3HT and CdSe(600) per mg of block copolymer. We refer to this system (Figure 7C) as "micelle I." TEM images of the micelle I system (for example, Figure 7A) show that QDs are bound to the surface of every micelle.

For comparison, we need a model system with a similar structure, but without the possibility of electronic energy transfer (EET) or photoinduced charge transfer (PCT) between the QDs and the P3HT. We assume that by confining the P3HT molecules and CdSe to different micelles, we increase the separation of these components, making EET and PCT much less likely to occur. For this purpose, we prepared a mixture of two micelles, one containing the *nr*-P3HT in the core with no QDs in the corona, and the other containing the CdSe(600) QDs in the corona, but no P3HT in the core. We refer to this mixture (Figure 7D) as "micelle II". For micelle II, TEM images (e.g., Figure 7B) show the coexistence of independent PS_{404}-*b*-$P4VP_{76}$ micelles, some of which can be seen to contain QDs. We assume that the apparently bare micelles contain P3HT in the core. The size of the bare micelles ($d = 33.4 \pm 4.3$ nm) is comparable to that of the QD-containing micelles ($d = 35.1 \pm 3.4$ nm). The coexistence of separate types of micelles seen in Figure 7B suggests that the exchange of QDs among micelles is not significant. Some bridging is observed, but this occurred as the sample dried on the TEM grid. The migration of P3HT from P3HT/PS-*b*-P4VP micelles to QDs/PS-*b*-P4VP micelles is unlikely because of the low solubility of P3HT in 2-PrOH and the steric effect of the P4VP corona.

In Figure 7E, we show that at identical concentrations of QDs and P3HT, there is complete overlap of the absorption spectra of micelle I and II at wavelengths above 520 nm. At lower wavelengths, higher optical density was observed in micelle II, presumably due to an enhanced contribution of light scattering. The most important result in Figure 7 is the demonstration in the steady-state fluorescence spectra (Figure

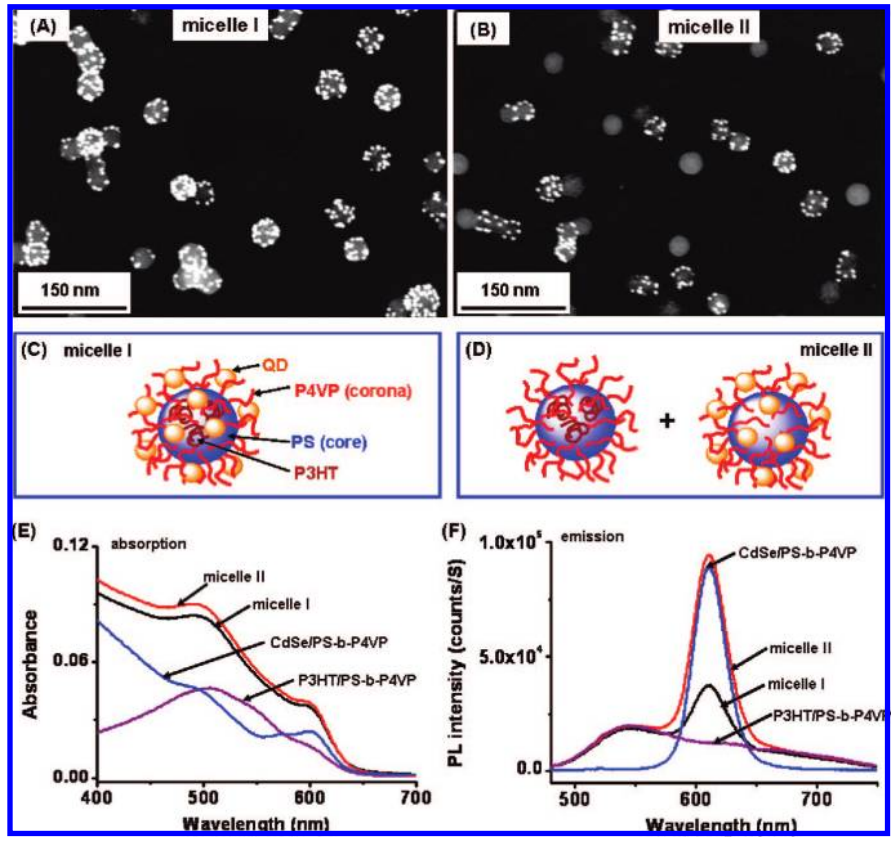

Figure 7. (A) TEM image of a sample of micelle I: PS_{404}-*b*-$P4VP_{76}$ micelles with CdSe(600) QDs in the corona and P3HT in the core. (B) TEM image of a sample of micelle II: a mixture of PS_{404}-*b*-$P4VP_{76}$ micelles with CdSe(600) QDs in the corona plus PS_{404}-*b*-$P4VP_{76}$ micelles with P3HT in the core. (C,D) A schematic presentation of micelle I and micelle II, respectively. (E) UV-vis absorption and (F) photoluminescence spectra (λ_{ex} = 450 nm) in 2-PrOH of micelle I and micelle II. The concentrations of QDs in the solution of micelle I and of micelle II were identical, as were the concentrations of P3HT. Also included for comparison are the absorption and emission spectra in 2-PrOH of PS-*b*-P4VP micelles containing P3HT and of PS-*b*-P4VP micelles containing CdSe(600) QDs. The concentrations of P3HT and of CdSe(600) QDs in these solutions match those in the solutions of micelle I and micelle II.

7F), that the CdSe(600) QDs in micelle I exhibit lower PL intensity at the band-edge maximum (615 nm) than those in the micelle II system, in which the QDs and P3HT are physically separated. This is clear evidence for excited-state quenching of the QDs, presumably by aggregates of P3HT, although we cannot at this time assign this quenching to EET or PCT.

As an additional control experiment, we prepared an additional solution of CdSe/PS-P4VP consisting of QD-loaded micelles without P3HT, matching the concentration of the micelles and QDs to that of micelle I. As one can see in Figure 7F, the PL intensity of this sample is very similar to that of micelle II, providing additional evidence that no PL quenching occurs in micelle II, in which the P3HT and QDs are confined to separate block copolymer micelles.

In addition, Figure 7F shows that the presence of the QDs has little effect on the weak residual emission of P3HT in micelle I. In Figure 4C, we show that aggregation of this polymer accompanying incorporation into the micelles led to loss of more than 99% of the emission intensity. The intensity of this residual P3HT emission for micelle I is comparable to that for micelle II. It is not known whether this is a weak emission from the aggregate or a competing emission from a trace amount of monomeric polymer.[46–48]

For PCT to occur, intimate contact is normally required between the electron donor and acceptor. In the description of the structure of the hybrid nanocomposite micelles, we provided evidence that the CdSe QDs were close to, and possibly in contact with, the surface of the micelle core. It is also possible, but at this time impossible to establish, that the P3HT itself may lie adjacent to the core-solvent interface. Thus, intimate contact is possible. However, the long tail in this emission of the P3HT seen in Figure 7F suggests that this conjugated polymer has states lower in energy than the QD. From this perspective, EET from electronically excited QDs to this polymer is also possible. In an attempt to learn more about the interaction mechanisms, we prepared micelles analogous to micelle I using core/shell CdSe/ZnS QDs with a PL maximum at 640 nm (Figure 8). We imagined that EET might be less sensitive to small changes in donor−acceptor distance than PCT. As shown in Figure 8B, the QD/PS_{404}-*b*-$P4VP_{76}$ micelles in the presence and absence of P3HT showed almost identical emission (Figure 8B) and excitation (Figure 8C) spectra, indicating that no quenching of the QD emission took place. The thin ZnS shell on the CdSe/ZnS QDs suppressed PL quenching of the QDs. This result provides some support to the idea that charge transfer may

(46) Österbacka, R.; An, C. P.; Jiang, X. M.; Vardeny, Z. V. *Science* **2000**, *287*, 839–842.
(47) Chen, T. A.; Wu, X.; Rieke, R. D. *J. Am. Chem. Soc.* **1995**, *117*, 233–244.
(48) Sirringhaus, H.; Brown, P. J.; Friend, R. H.; Nielsen, M. M.; Bechgaard, K.; Langeveld-Voss, B. M. W.; Spiering, A. J. H.; Janssen, R. A. J.; Meijer, E. W.; Herwig, P.; Leeuw, D. M. d. *Nature* **1999**, *401*, 685–688.

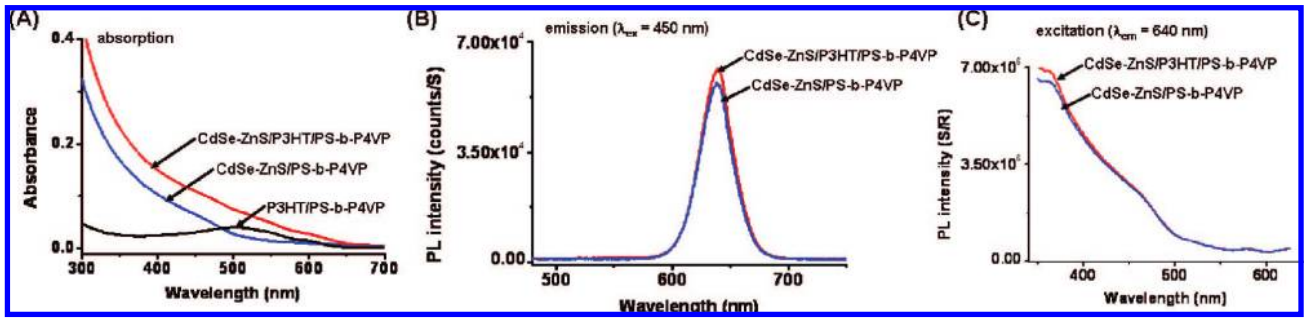

Figure 8. UV−visible absorption (A), emission (B), and excitation (C) spectra, respectively, of the PS_{404}-*b*-$P4VP_{76}$ micelles with either *nr*-P3HT at the core or core/shell CdSe/ZnS QDs at the corona or with both components in 2-PrOH. The concentration of PS-*b*-P4VP in all the samples is 0.25 mg/mL.

contribute to the quenching process for samples of micelle I containing CdSe QDs. Alternatively, Burda et al.[49,50] reported that the energy transfer efficiency from CdSe/ZnS core/shell QDs to phthalocyanine acceptor molecules was significantly lower than that for bare CdSe QDs. They also presented evidence that the EET did not follow the traditional Förster mechanism. In addition, Vinayakan et al.[51] demonstrated that two monolayers of a ZnS shell prevented electron transfer from the CdSe core to phenothiazine as a hole scavenger. Both of these studies are consistent with our observation that the ZnS shell affects the excited-state interaction between CdSe/ZnS core/shell QDs and P3HT.

Our goal in carrying out these experiments was to create a system with a spatially defined organization of multiple functional materials, i.e., QDs and conjugated polymers, using polymeric micelles as a template. Further experiments are needed to establish the details of the quenching mechanism. Nonetheless, it is interesting to note that, just as in many natural light harvesting systems, chromophore aggregates play a role in trapping electronic excitation.

Conclusions

We have reported a simple, effective approach to achieving a spatially defined organization of colloidal QDs with poly(3-hexylthiophenes), using crew-cut micelles of a PS_{404}-*b*-$P4VP_{76}$ block copolymer as the main structural motif. We were able to generate this colloidal hybrid nanocomposite from a solution of the components in a common good solvent. Self-assembly was triggered by the addition of an alcohol as a selective precipitant. Most experiments were carried out with 2-PrOH as the medium. Experiments with other alcohols (butanol, methanol) indicated that these solvents influenced the size of the micelles formed by PS_{404}-*b*-$P4VP_{76}$. Thus, in the future, one can imagine using the choice of solvent as well as polymer composition as strategies for manipulating the detailed structure of colloidal composites like those shown in Chart 1.

The concept presented here of integrating two functional components into a single polymeric micelle with spatially defined organization is also applicable to more than two components. For example, colloidal QDs with different sizes and shapes or even other metal or metal oxide nanocrystals can be attached to the micelles. Moreover, other organic functionalities such as organic dyes and other conjugated polymers which show selective solubility can be encapsulated into the polymeric micelles. Shape control of the micellar templates is also possible owing to the rich self-assembling morphologies of block copolymers in solution and in the solid state. Thus, our approach offers considerable flexibility for preparing a range of nanocomposites with both integrated multiple functions and ordered hierarchical organization, reminiscent of structures of light harvesting complexes in nature. For example, the block copolymer forms a higher order structure—the micelle—that serves as a scaffold for organizing the light-absorbing components. The conjugated polymers are incorporated into the core of each micelle via hydrophobic interactions, while the QDs are tethered by ligand groups built into the micelle corona domain.

Significantly, the micellar systems we reported here are substantially larger than most natural light harvesting proteins. Each QD, for example, is similar in size to the entire LH2 complex. One consequence of this size difference might be the greatly diminished efficiency of EET or PCT in micelle I compared to natural systems comprising organized molecular chromophores. We anticipate that the spatially defined organization of the active components in the present system will provide new opportunities for studying the complicated photophysics intrinsic to blends of nanoscale systems, such as bulk heterojunctions, which are characterized by electronic interactions at interfaces rather than between specific donor−acceptor molecules.

Acknowledgment. The authors thank the Natural Sciences and Engineering Research Council of Canada for support of this research. G.D.S. acknowledges the support of an E. W. R. Steacie Memorial Fellowship. We are grateful to Evident Technologies for the gift of the core/shell CdSe/ZnS QDs. We also thank W. Lin for the help in the PL measurement of PbS QDs and thank Prof. E. H. Sargent for the use of his instrument.

Supporting Information Available: Information about the experimental materials and methods, ^{1}H NMR spectra of PS_{404}-*b*-$P4VP_{76}$ in $CDCl_3$ and in $CDCl_3$/CD_3OD (1:2 v/v), TEM images of PS_{404}-*b*-$P4VP_{76}$ micelles and micelle−CdSe(559) complexes formed in $CHCl_3$/CH_3OH (1:2 v/v); of CdSe(600)/P4VP (or P2VP)/PS_{404}-*b*-$P4VP_{76}$ micelles in 2-PrOH; of PS_{404}-*b*-$P4VP_{76}$ micelles and micelle−CdSe(600) complexes formed in 2-PrOH; of PS_{404}-*b*-$P4VP_{76}$ micelles containing P3HT (20 and 400 μg/mg block copolymer). Also, absorption and emission spectra of *rr*-P3HT in $CHCl_3$ and of PS_{404}-*b*-$P4VP_{76}$ micelles in 2-PrOH containing P3HT;

(49) Dayal, S.; Lou, Y. B.; Samia, A. C. S.; Berlin, J. C.; Kenney, M. E.; Burda, C. *J. Am. Chem. Soc.* **2006**, *128*, 13974–13975.
(50) Dayal, S.; Burda, C. *J. Am. Chem. Soc.* **2007**, *129*, 7977–7981.
(51) Vinayakan, R.; Shanmugapriya, T.; Nair, P. V.; Ramamurthy, P.; Thomas, K. G. *J. Phys. Chem. C* **2007**, *111*, 10146–10149.

TEM and SEM images of dried droplets of the mixture of P3HT, CdSe(600)/TOPO and PS_{404}-*b*-$P4VP_{76}$ in $CHCl_3$; a TEM image and absorption and emission spectra of CdSe(600)/TOPO from toluene; absorption and emission spectra of a mixture of CdSe(600)/TOPO and PS_{404}-*b*-$P4VP_{76}$ in $CHCl_3$ compared with those of their composite micelles in 2-PrOH; and absorption spectra of CdSe(600)/P3HT/PS_{404}-*b*-$P4VP_{76}$ composite micelles in 2-PrOH for different ratios of QDs to block copolymer. This material is available free of charge via the Internet at http://pubs.acs.org.

JA801931M